Published in final edited form as:
Neurobiol Dis. 2008 October ; 32(1): 142–150. doi:10.1016/j.nbd.2008.07.006.

JNK is activated but does not mediate hippocampal neuronal apoptosis in experimental neonatal pneumococcal meningitis

Matthias D. Sury[1], **Claudia Agarinis**[1], **Hans-Rudolf Widmer**[2], **Stephen L. Leib**[1], and **Stephan Christen**[1]

[1]*Institute of Infectious Diseases, University of Berne, CH-3010 Berne, Switzerland* [2]*Department of Neurosurgery, University of Berne, Berne, Switzerland*

Abstract

Pneumococcal meningitis is associated with caspase 3-dependent apoptosis of recently post-mitotic immature neurons in the dentate gyrus of the hippocampus. The death of these cells is implicated in the learning and memory deficits in patients surviving the disease. The stress-activated protein kinase c-Jun N-terminal kinase (JNK) has been shown to be an important mediator of caspase 3-dependent neuronal apoptosis. However, whether JNK is involved in hippocampal apoptosis caused by pneumococcal meningitis has not been investigated so far. Here we show in a neonatal rat model of pneumococcal meningitis that JNK3 but not JNK1 or JNK2 is activated in the hippocampus during the acute phase of infection. At the cellular level, JNK3 activation was accompanied in the dentate gyrus by markedly increased phosphorylation of its major down-stream target c-Jun in early immature (Hu-positive) neurons, but not in migrating (doublecortin-positive) neurons, the cells that do undergo apoptosis. These findings suggested that JNK may not be involved in pneumococcal meningitis-induced hippocampal apoptosis. Indeed, although intracerebroventricular administration of D-JNKI-1 or AS601245 (two highly specific JNK inhibitors) inhibited c-Jun phosphorylation and protein expression in the hippocampus, hippocampal apoptosis was unaffected. Collectively, these results demonstrate that JNK does not mediate hippocampal apoptosis in pneumococcal meningitis, and that JNK may be involved in processes unrelated to apoptosis in this disease.

Keywords

neuronal apoptosis; bacterial meningitis; dentate gyrus; c-Jun N-terminal kinase; D-JNKI-1; AS601245

Introduction

Bacterial meningitis caused by *Streptococcus pneumoniae* (”pneumococcus”), a severe infectious disease of the central nervous system, remains to be associated with high mortality and morbidity rates, despite the advances made in antimicrobial therapy over the past decades (Merkelbach et al., 2000; Schuchat et al., 1997). One of the consequences of the massive inflammatory reaction in the meninges and subarachnoid space is the occurrence of neuronal

Address correspondence to: Dr. Stephan Christen, Institute of Infectious Diseases, Friedbuehlstrasse 51, CH-3010 Berne, Switzerland. Phone: +41 (31) 632 8707; Fax: +41, (31) 632 3550; E-mail: stephan.christen@ifik.unibe.ch.

apoptosis in the hippocampus (Braun et al., 1999). The death of these cells appears to be responsible for the learning and memory deficits in patients surviving the disease (Grimwood et al., 1995; Leib et al., 2001; Nau et al., 1999). Thus, in experimental pneumococcal meningitis, the extent of hippocampal apoptosis correlates with the extent of learning dysfunction (Leib et al., 2001; Loeffler et al., 2001). The cells undergoing apoptosis in pneumococcal meningitis are located in the subgranular zone (SGZ) of the hippocampal dentate gyrus and have been identified in animal models to be recently postmitotic immature neurons, based on BrdU labeling experiments and the finding that they are positive for MAP2 but negative for the mature neuronal marker NeuN (Bifrare et al., 2003; Grandgirard et al., 2007). During development of the brain (and to some extent in the adult brain), newly formed neurons derived from progenitor cells located in the SGZ migrate into the granular layer of the dentate gyrus, where they become integrated and differentiate into mature neurons.

Hippocampal neuronal apoptosis in pneumococcal meningitis has been shown to be almost exclusively caspase 3-dependent (Gianinazzi et al., 2003; Mitchell et al., 2004). However, the pathways that lead to caspase 3 activation and hence apoptosis in pneumococcal meningitis have not been identified so far. The stress-activated protein kinase c-Jun N-terminal kinase (JNK) has been shown to be an important mediator of caspase 3-dependent apoptosis. JNK can be involved in the activation of caspase 3 both during death receptor-mediated apoptosis and apoptosis mediated by the mitochondrial pathway (Papa et al., 2004; Weston and Davis, 2007). JNK has been shown to mediate neuronal apoptosis in a variety of stress conditions. Thus, neuronal apoptosis induced by growth factor withdrawal (Cao et al., 2004; Eilers et al., 2001; Xia et al., 1995) or excitatory amino acids (Borsello et al., 2003; Eminel et al., 2007) was shown to be JNK dependent. Furthermore, treatment with pharmacological JNK inhibitors reduces neuronal apoptosis in rodent models of cerebral ischemia (Borsello et al., 2003; Carboni et al., 2004; Okuno et al., 2004) and viral encephalitis (Beckham et al., 2007). Finally, caspase 3 activation in the dentate gyrus by the gram-negative cell wall component lipopolysaccharide is mediated by JNK (Barry et al.). These findings prompted us to investigate the role of JNK in hippocampal neuronal apoptosis caused by pneumococcal meningitis.

The different JNK isoforms (JNK1, 2, and 3) appear to be involved in different kinds of neuronal apoptosis (Manning and Davis, 2003; Waetzig and Herdegen, 2005). While JNK1 and 2 has been shown to be important for apoptosis in early brain development (Chang et al., 2003; Kuan et al., 1999), JNK3 has been implicated in neuronal apoptosis induced by excitatory amino acids or cerebral ischemia (Brecht et al., 2005; Kuan et al., 2003; Yang et al., 1997). However, the different JNK isoforms (including JNK3) do not only have pro-apoptotic activity, but also mediate neuronal differentiation and neuritogenesis (Manning and Davis, 2003; Waetzig and Herdegen, 2005).

To investigate the role of JNK in hippocampal apoptosis caused by pneumococcal meningitis, we determined the expression pattern and phosphorylation status of the major JNK downstream target c-Jun, and the isoform-specific activation status of JNK in the hippocampus, and the effect of JNK inhibition in a well-characterized neonatal rat model of pneumococcal meningitis (Gianinazzi et al., 2003; Grandgirard et al., 2007; Pfister et al., 2000).

Materials and Methods

Neonatal rat model of pneumococcal meningitis

Eleven day old Wistar rats (22–24 g) were intracisternally infected with 10 μl of saline containing 2 × $\log_{10}$ 6 cfu/ml of *S. pneumoniae* P21, or were mock-infected with 10 μl sterile saline. Eighteen hours post infection (p.i.), animals were clinically assessed using the following scale of scores: 1 = coma; 2 = does not turn upright; 3 = turns upright within 30 sec; 4 = minimal ambulatory activity, turns upright in less than 5 sec; 5 = normal. Animals with a score of 2 or

below were immediately sacrificed for ethical reasons. Additionally, cerebrospinal fluid (CSF) was obtained by puncture of the cisterna magna and quantitatively assessed for bacterial growth by plating serial dilutions on Columbia sheep blood agar plates. After CSF sampling, animals received intraperitoneal ceftriaxone (100 mg/kg; Roche Pharma, Reinach Switzerland) to resolve the infection. Animals were sacrificed by decapitation at the indicated time points and brains processed as described below. Animal experiments were approved by the Animal Care and Experimentation Committee of the Canton of Berne (Switzerland) and strictly followed the National Institute of Health's guidelines for the performance of animal experiments.

Inhibitor treatment

Animals were anesthetized intraperitoneally with 50 mg/kg ketamine and 0.2 mg/kg medetomidine and positioned in a stereotaxic frame (Kopf Model 900 Small Animal Stereotaxic Instrument, Tujunga, CA) with an adaptor for neonatal rats (Kopf Model 970 Neonatal Rat Adapter). The scalp was incised on the midline and the skull exposed. D-JNKI-1 and D-TAT control peptide (4 nmol each, kindly provided by Xigen S.A.) dissolved in PBS, or AS601245 (200 nmol, Calbiochem, San Diego, CA) dissolved in DMSO were injected intracerebroventricularly (i.c.v.) into the lateral ventricle of each hemisphere 4 h before infection. Drug infusion was performed using a 10-μl Hamilton syringe (Hamilton, Bonaduz, Switzerland), 2.0 mm laterally, 0.3 mm posteriorly and 3.2 mm deep relative to bregma at a rate of 1 μl/min. Using this procedure, FITC-labeled D-TAT was readily taken up by the hippocampus. The concentrations of the two inhibitors were chosen based on reported values in the literature (Borsello et al., 2003; Carboni et al., 2005; Carboni et al., 2004; Zhuang et al., 2006) and on initial dose-finding experiments looking at the effect on c-Jun phosphorylation.

Histopathological evaluation of apoptosis

Animals were killed 24 h p.i. and a brain hemisphere fixed for 24 h at 4°C with 4% phosphate-buffered paraformaldehyde. The contralateral hemisphere was used for analyzing biochemical parameters as described below. Fixed brain hemispheres were cryo-preserved at 4°C in 18% sucrose, shock-frozen in 2-methylbutane, and 45 μm thick coronal sections were cut on a Cryostat (Jung CM1800, Leica, Glattbrugg, Switzerland). Four sections of the dorsal brain region (region 1 to 4, each ~600 μM apart, spanning the entire depth of the dentate gyrus) were mounted on polylysine-coated slides, stained for Nissl bodies with cresyl violet, and cells with morphological features of apoptosis (i.e., condensed fragmented dark nuclei and apoptotic bodies, cf. Figure 5A) were counted in the upper and the lower blade of the dentate gyrus as described previously (Pfister et al., 2000). Cells with apoptotic morphology are ~90% positive for active caspase 3 (Gianinazzi et al., 2003). Apoptotic cells were counted by an investigator blinded to the experiment.

Western blot analysis

Western blot analysis of phosphorylated proteins was performed as described previously (Sury et al., 2006) with the following modifications. Hippocampi were dissected in ice-cold PBS and stored at −80°C until analysis. Tissue was homogenized in modified radio-immunoprecipitation (RIPA) buffer (50 mM Tris HCl pH 7.4, 150 mM NaCl, 1% NP-40, 0.25% Na-deoxycholate, 1 mM EDTA) containing 0.1% sodiumdodecylsulfate (SDS), and the following protease and phosphatase inhibitors: Aprotinin 1 μg/ml, leupeptin 1 μg/ml, pepstatin 1 μg/ml, 1 mM sodium fluoride, 1 mM sodium orthovanadate, 20 mM sodium pyrophosphate, 1X phosphatase inhibitor cocktail 1 (all from Sigma-Aldrich, St. Louis, USA) and phenylmethyl sulfonyl fluoride (Calbiochem, San Diego, CA). Protein concentration was determined using a BCA protein assay kit (Pierce, Rockford, IL). Equal amounts of protein were separated under reducing conditions on a 10% SDS polyacrylamide gel (Bio-Rad Laboratories, Hercules, CA). After blotting onto a nitrocellulose membrane (Macherey-Nagel,

Düren, Germany), non-specific binding sites were blocked for 2 hours with 5% non-fat dry-milk in Tris-buffered saline containing 0.1% Tween 20. The membrane was incubated overnight using antibodies against either phospho-c-Jun Ser73 or c-Jun (both from Cell Signaling Technologies, Beverly, MA, 1:1000). Horseradish peroxidase-conjugated mouse anti-rabbit antibody (Sigma, 1:20'000) was used as secondary antibody. Reprobing with an antibody against β-actin (Sigma, 1:10'000) was used to verify equal protein loading. Blots were incubated with peroxidase chemiluminescence substrate (Millipore, Billerica, MA or Pierce, Rockford, IL) and signals detected on Fuji medical x-ray film (Fuji Photo Film, Tokyo, Japan). For densitometric analysis, band intensities were determined with the PC version of NIH image (Scion Corporation, Frederick, MD).

JNK immunoprecipitation

Tissue was homogenized under non-denaturing conditions in ice-cold immunoprecipitation (IP) lysis buffer (50 mM Tris HCl pH 7.4, 150 mM NaCl), 1% Triton X-100, 1 mM EDTA, 1 mM EGTA) containing protease and phosphatase inhibitors as described above. Protein concentration was measured by Bradford assay (Sigma). Samples were diluted with IP lysis buffer to a protein concentration of 1 mg/ml. For each IP, 500 µl of sample was incubated overnight with 0.5 µg rabbit anti-JNK3 monoclonal antibody (Upstate, Lake Placid, NY) at 4°C on a turning wheel. After incubation with protein A-sepharose beads (50% slurry, EZview Red Protein A Affinity Gel, Sigma), the supernatant was removed and used for Western Blot analysis. To release the immunocomplexes from the beads, SDS-PAGE loading buffer (50 mM Tris-HCl, pH 6, 2% SDS, 10% glycerol) was added and samples were boiled at 95°C for 5 min. After adding bromphenol blue, equal amounts of protein sample were loaded on a 10% polyacrylamide SDS gel, blotted onto a nitrocellulose membrane and incubated with the following primary antibodies: Mouse monoclonal anti-phospho-JNK antibody (Cell Signaling Technology, Beverly, MA, 1:2000), rabbit monoclonal anti-JNK3 antibody (Upstate, Lake Placid, NY, 1:2000), mouse monoclonal anti-JNK1/2 antibody (BD PharMingen, Franklin Lakes, NJ, 1:2000). As secondary antibodies, horseradish peroxidase-conjugated goat anti-mouse IgG antibody (Sigma, 1:20'000) and light chain-specific horseradish peroxidase-conjugated mouse anti-rabbit IgG, antibody (Jackson ImmunoResearch Laboratories, West Grove, PA, 1:10'000) were used.

JNK3 kinase activity

Preparation of protein extracts and IP were performed as described above. Following IP, kinase buffer (25 mM Tris HCl, pH 7.4, 2 mM dithiotreitol, 10 mM $MgCl_2$, 0.1 mM sodium orthovanadate, 5 mM glycerol-2-phosphate, 2.5 mM sodium pyrophosphate (all from Sigma) and c-Jun protein/ATP mixture (Biovision, Mountain View, CA) was added to the washed protein A beads and incubated for 1 h at 30°C. The reaction was stopped with SDS-PAGE loading buffer and analyzed by Western blotting.

Immunofluorescence

Animals were killed by cervical dislocation 24 h after infection and immediately perfused with 4% phosphate-buffered paraformaldehyde. Brains were removed from the skull and fixed for 24 h in 4% paraformaldehyde containing phosphatase inhibitor cocktail 1 (Roche, Basel, Switzerland). After incubation in 50% ethanol for 48 h, brains were embedded in paraffin and 6 µm coronal sections cut on a microtome. Sections were deparaffinized in xylene and rehydrated, followed by antigen unmasking by boiling for 10 min in 10 mM sodium citrate buffer, pH 6.0. Tissue sections were blocked with 10% normal goat serum (Sigma) for 2 h and incubated over night at 4°C with either rabbit polyclonal anti-phospho-c-Jun (Ser73) antibody (Cell Signaling, Technology, Beverly, MA), rabbit monoclonal anti-cleaved caspase 3 (Asp175) antibody (Cell Signaling, Technology, Beverly, MA), mouse monoclonal anti-NeuN

antibody (Chemicon International, Temecula, CA) or mouse monoclonal anti-Hu antibody (Santa Cruz Biotechnology, Santa Cruz, CA) at dilutions of 1:400, 1:400, 1:1000 and 1:400, respectively. This was followed by incubation with Alexa Fluor 555 goat anti-rabbit IgG and Alexa Fluor 488 goat anti-mouse IgG secondary antibodies (Invitrogen Corporation, Carlsbad, CA) at dilutions of 1:1000 for 2 h. Co-staining with goat anti-doublecortin at a dilution of 1:1000 (Santa Cruz Biotechnology, Santa Cruz, CA) and either anti-phospho-c-Jun (Ser73) antibody or anti-cleaved caspase 3 (Asp175) antibody was performed using 10% donkey serum for blocking and Alexa Fluor 555 donkey anti-rabbit IgG and Alexa Fluor 488 donkey anti-goat IgG as secondary antibodies (Invitrogen Corporation, Carlsbad, CA) at dilutions of 1:1000. The sections were counterstained with 4',6-diamidino-2-phenylindol (DAPI) and mounted with ProLong Gold antifade (Invitrogen). Non-specific staining was assessed by incubation of sections in the absence of primary antibodies. Images were taken with a digital camera (Hamamatsu, Japan) and processed using OpenLab 4.0.3 imaging analysis software (Improvision, Coventry, England) as described previously (Ren et al., 2007; Schaper et al., 2002).

In situ labeling of DNA fragmentation

Terminal deoxynucleotidyl transferase-mediated nick end-labeling (TUNEL) staining was performed after immunostaining using the Fluorescein FragEL™ DNA Fragmentation Detection Kit (Calbiochem) according to the manufacturer's protocol. Sections were incubated with deoxynucleotidyl transferase and fluorescein-labeled deoxynucleotides for 2 h at 37°C and mounted with ProLong Gold antifade reagent (Invitrogen).

Myeloperoxidase (MPO) activity

Five µl of CSF was centrifuged for 5 min at 500 × g at 4°C and the resulting pellet stored at −80°C until analysis of MPO activity as described previously (Christen et al., 2001).

Statistical analysis

Student t test was used for comparison between two groups and ANOVA followed by Bonferroni post hoc test for comparisons between multiple groups (Prism 4.0, GraphPad Software, San Diego, CA). Data are presented as mean ± SE in experiments where data are compared relative to a control group (=100%), while SD was used for presenting absolute numbers (Cumming et al., 2007). A P-value <0.05 was considered to be statistically significant. The numbers of animals used for each experiment are described in the result section or the corresponding figure legend.

Results

Experimental neonatal pneumococcal meningitis is associated with increased c-Jun phosphorylation and JNK3 activity in the hippocampus

To see whether JNK is activated during pneumococcal meningitis, hippocampal homogenates prepared at different time points after infection were analyzed for both phospho-c-Jun (Ser73) and total c-Jun protein. Western blot analysis revealed that c-Jun becomes progressively phosphorylated during infection, and that this increase in phosphorylation is accompanied by upregulation of c-Jun protein in the hippocampus (Fig. 1A). c-Jun phosphorylation and protein levels returned to pre-infection values at 40 h after infection (data not shown).

To investigate which JNK isoform is responsible for increased c-Jun phosphorylation in the hippocampus, we performed an isoform-specific analysis of JNK activation using antibodies directed against the dual-phosphorylation site required for kinase activation. Hippocampal homogenates prepared at different time points after infection were subjected to

immunoprecipitation using a JNK3-specific antibody. As shown in Figure 1B, the JNK3 antibody completely precipitated JNK3 from the homogenates and left JNK1 and 2 in the supernatant. Subsequent analysis of these two fractions revealed that pneumococcal meningitis is associated with increased phosphorylation of JNK3 but not of JNK1 or 2. To see whether increased JNK3 phosphorylation was also associated with increased JNK3 activity, JNK3 immunoprecipitates were analyzed for in vitro kinase activity using GST-c-Jun as substrate. Indeed, the infection-associated increase in JNK3 phosphorylation was accompanied by increased JNK3 kinase activity (Fig. 1C). These results strongly suggest that the increase of c-Jun phosphorylation in the hippocampus during infection is mediated by JNK3.

c-Jun phosphorylation is markedly increased in early immature neurons of the dentate gyrus but does not co-localize with apoptotic cells

Pneumococcal meningitis primarily caused an increase of c-Jun phosphorylation in the dentate gyrus of the hippocampus, the region where neuronal apoptosis occurs during this disease (Fig. 2A, B). Double-staining with NeuN (a marker of mature neurons) revealed that c-Jun phosphorylation was markedly induced in cells of the subgranular zone (SGZ) but only weakly in neurons of the granular cell layer (Fig. 2C, D). To further characterize the identity of the phospho-c-Jun-positive cells, we performed double-staining experiments with differentiation-specific neuronal markers (Gleeson et al., 1999; Jin et al., 2001; Wakamatsu and Weston, 1997) and/or markers of apoptosis. Increased phospho-c-Jun staining was almost exclusively observed in Hu-positive (i.e., early immature), but not migrating (i.e., doublecortin-positive) neurons (Fig. 2E, F). However, Hu-positive cells did not show any co-localization with active caspase 3 (Fig. 3A). Active caspase 3-positive cells were often found to be doublecortin-positive (Fig. 3B). Furthermore, phospho-c-Jun-positive cells did not co-localize with TUNEL-positive cells (Fig. 3C), strongly suggesting that JNK, although activated, is not involved in pneumococcal meningitis-induced hippocampal apoptosis.

Intracerebroventricular treatment with D-JNKI-1 or AS601245 inhibits the infection-associated increase in c-Jun phosphorylation and protein expression, but has no effect on hippocampal apoptosis

To verify that JNK is not involved in hippocampal apoptosis, we used two different highly specific JNK inhibitors, previously shown to inhibit neuronal apoptosis in models of cerebral ischemia (Borsello et al., 2003; Carboni et al., 2004) and viral encephalitis (Barry et al., 2005). To be able to concurrently determine c-Jun phosphorylation and hippocampal apoptosis, the effect of JNK inhibition was analyzed at 24 h p.i, a time point at which apoptosis is near the maximum (Gianinazzi et al., 2003). Treatment with D-JNKI-1, a peptide inhibitor that blocks interaction of JNK with its substrates and activators, effectively blocked increased c-Jun phosphorylation in the dentate gyrus (Fig. 4A), indicating that pneumococcal meningitis-induced c-Jun phosphorylation in the hippocampus is mediated by JNK. By Western blot analysis (Fig. 4B), hippocampal c-Jun phosphorylation and upregulation of c-Jun protein were significantly inhibited by 48 ± 10 and 47 ± 11%, respectively (both $P < 0.05$, 10 D-JNKI-1-treated vs. 6 D-TAT-treated animals). However, D-JNKI-1 treatment had no effect on pneumococcal meningitis–induced hippocampal apoptosis compared to vehicle-treated animals (Fig. 5A and B). Treatment with D-JNKI-1 had no effect on apoptosis in mock-infected animals (0.0 ± 0.0, n=3 vs. 0.04 ± 0.05 in D-TAT-treated animals, n=4, $P > 0.05$). The lack of effect of D-JNKI-1 cannot be explained by an altered host response against the pneumococcal infection, as treatment with D-JNKI-1 had no effect on CSF bacterial titers, clinical score, weight loss and CSF MPO activity (as an index of granulocyte infiltration, (Krawisz et al., 1984)) (Table 1). Albeit, treatment with vehicle (D-TAT) appeared to have a slight effect on the number of apoptotic cells in the hippocampus compared to animals injected with saline (64.2 ± 14.4 vs. 44.8 ± 8.3, n=4 each, $P > 0.05$).

To corroborate the findings with D-JNKI-1, we also used the structurally different JNK inhibitor AS601245, which blocks JNK activity by binding to its ATP-binding site. Like D-JNKI-1, i.c.v. treatment with AS601245 effectively inhibited c-Jun phosphorylation in the dentate gyrus when evaluated by immunofluorescence (not shown). By Western blot analysis, hippocampal c-Jun phosphorylation and protein expression were significantly inhibited by 40 ± 10 and 80 ± 22%, respectively (both $P < 0.05$, 11 AS601245-treated vs. 10 vehicle-treated infected animals) (Fig. 6A). Again, JNK inhibition had no effect on hippocampal apoptosis (Fig. 6B) and no effect on the clinical course of infection (Table 1). AS601245 treatment had no effect on apoptosis in mock-infected animals (0.08 ± 0.14, n=3 vs. 0.31 ± 0.54 in vehicle-treated animals, n=4, P>0.05).

Discussion

In this study, we found that pneumococcal meningitis in infant rats leads to marked induction of c-Jun phosphorylation and c-Jun protein expression in the hippocampus, a brain region afflicted by neuronal apoptosis during this disease. c-Jun activation was accompanied by activation of JNK3 but not of JNK1/2, strongly suggesting that increased phosphorylation of c-Jun was mediated by JNK3. Activation of c-Jun was most prominent in the dentate gyrus, the region where immature neurons undergo apoptosis in pneumococcal meningitis. However, increased phosphorylation of c-Jun occurred in a subpopulation of immature neurons (Hu-positive, early immature neurons) that do not co-localize with markers of apoptosis, while doublecortin-positive (migrating) neurons, which co-localize with markers of apoptosis, do not show any increase in c-Jun phosphorylation. Furthermore, there was no overlap between TUNEL and phospho-c-Jun-positive cells. These immunohistochemical findings strongly suggested that JNK may not be involved in hippocampal apoptosis. We therefore applied the two highly specific JNK inhibitors D-JNKI-1 and AS601245, which inhibited the infection-associated increase in c-Jun phosphorylation, but had no effect on hippocampal apoptosis. Thus, our results provide clear evidence that in contrast to other models of acute brain injury JNK does not mediate hippocampal apoptosis in pneumococcal meningitis.

The cells that undergo apoptosis during pneumococcal meningitis have recently been identified to be recently post-mitotic immature neurons (Grandgirard et al., 2007). Co-localization between BrdU and active caspase 3 revealed that these cells underwent mitosis 6–10 days before pneumococcal meningitis. In addition, apoptotic cells were positive for the neuronal marker MAP2, but negative for the mature neuronal marker NeuN, indicating that the neurons are not yet fully differentiated. In our study, we found that pneumococcal meningitis induced a marked increase in c-Jun phosphorylation in the SGZ of the dentate gyrus, the region where cells undergo apoptosis. The inhibitor experiments clearly show that this increase in c-Jun phosphorylation is JNK-dependent. To identify the cell type in which JNK was activated (most likely the JNK3 isoform), we used different developmental stage-dependent neuronal markers. Intriguingly, we found that the most prominent increase in c-Jun phosphorylation occurred almost exclusively in early immature neurons, characterized by the expression of Hu RNA-binding proteins, which are involved in early differentiation of recently post-mitotic neurons (Wakamatsu and Weston, 1997). However, these cells were neither positive for active caspase 3 or TUNEL, nor showed any morphological evidence of apoptosis (condensed and/or fragmented nuclei). Since apoptotic cells may loose their differentiation markers, we may not have been able to see co-localization between Hu and apoptosis. However, the fact that D-JNKI-1 and AS601245 inhibited JNK in these cells (as evidenced by the marked inhibition of c-Jun phosphorylation), but had no effect on apoptosis, clearly demonstrates that JNK activation does not lead to apoptosis in these cells. Conversely, the cell population that is vulnerable to apoptosis (i.e., doublecortin-positive, migrating neurons) do not exhibit an increase in c-Jun phosphorylation, which together with the lack of effect of JNK inhibition clearly indicates that JNK is not involved in apoptosis of these cells.

JNK was inhibited *in vivo* using two differently acting inhibitors. D-JNKI-1 consists of the minimal JNK binding domain sequence of JNK interacting protein-1 (JIP-1) and a HIV-TAT sequence that promotes cellular uptake, and inhibits JNK in an ATP non-competitive fashion. Intracerebroventricular injection of D-JNKI-1 readily inhibited the infection-associated increase in c-Jun phosphorylation and increase in c-Jun protein expression. Since D-TAT appeared to have a slight effect on hippocampal apoptosis and the specificity of D-JNKI-1 toward the different isoforms of JNK is not completely understood, we used the second-generation ATP-competitive JNK inhibitor AS601245 to corroborate the findings with D-JNKI-1. This inhibitor is highly specific towards JNK (Gaillard et al., 2005) and is known to have a similar selectivity against the different isoform (IC_{50} in μM: 0.15 [JNK1], 0.22 [JNK2], 0.07 [JNK3]). In our experiments, the two inhibitors specifically inhibited JNK activity in the hippocampus and had no effect on the clinical course of infection. Thus, neither of the inhibitors had an effect on systemic disease symptoms (clinical score, infection-induced weight loss) or CSF parameters linked to the incidence of hippocampal apoptosis (bacterial titer, granulocyte infiltration). This clearly demonstrates that the lack of effect of JNK inhibition on hippocampal apoptosis cannot be explained by a systemic side effect of the inhibitors.

Previous findings and preliminary results rather suggest that growth factor withdrawal or impaired pro-survival signaling is responsible for hippocampal apoptosis in pneumococcal meningitis. Unlike mature neurons, developing neurons undergo apoptosis if they do not receive extrinsic growth factor signals (Benn and Woolf, 2004). Growth factors such as brain-derived neurotrophic factor or nerve growth factor activate the phosphatidylinositol 3,4,5-triphosphate-dependent Akt survival pathway, which negatively regulates pro-apoptotic downstream targets such as Bad, p53 or Forkhead transcription factors. A possible involvement of growth factor signaling in hippocampal apoptosis (or lack thereof) is suggested by the fact that exogenous brain-derived neurotrophic factor inhibits caspase 3-dependent hippocampal apoptosis in experimental pneumococcal meningitis (Bifrare et al., 2005). Furthermore, we have preliminary experiments showing that hippocampal apoptosis is accompanied by a decrease in hippocampal phosphatidylinositol 3,4,5-triphosphate and phosphorylation of Akt. Restoration of Akt phosphorylation by inhibition of PTEN, a phosphatase that counterbalances phosphatidylinositol 3,4,5-triphosphate-dependent Akt activation, decreases apoptosis in the dentate gyrus (Sury et al., unpublished results). Collectively, theses findings suggest that hippocampal apoptosis in pneumococcal meningitis is not the result of cytokine-activated JNK-dependent death receptor signaling, but a consequence of impaired, JNK-independent cell survival signaling.

We can presently only speculate on the function of the JNK activation in the Hu-positive neurons. Apart from being involved in neuronal apoptosis, the different JNK isoforms have also been shown to be important mediators of neuronal differentiation and migration (Waetzig and Herdegen, 2005). Experiments in knock-out animals have revealed that all JNK isoforms are important for normal neuronal development (Eminel et al., 2007). Since the acute phase of pneumococcal meningitis is followed by increased neurogenesis (Gerber et al., 2003), it is possible that JNK may be involved in the initiation of a repair process early after injury. This area clearly warrants further investigation.

In summary, the results presented in this study demonstrate that JNK is activated in early immature hippocampal neurons during experimental neonatal pneumococcal meningitis. However, unlike in other models of acute brain injury, JNK activation is not involved in hippocampal apoptosis, since the cells undergoing apoptosis (which we have identified to be migrating neurons) do not show any evidence of activation. More importantly, JNK inhibition has no effect on hippocampal apoptosis. The functional role of the JNK activation in the Hu-positive neurons remains to be determined.

Acknowledgments

We thank Corinne Siegenthaler and Kevin Oberson for excellent technical assistance. We would also like to thank Dr. Christophe Bonny from Xigen SA, Lausanne, Switzerland for providing us with D-JNKI-1 and D-TAT control peptide. This study was supported by the Swiss National Science Foundation (grants 310000-108236, 31-116257, and 31000-120725) and the National Institute of Neurological Disorders and Stroke (R01 grant NS33997-10A).

References

Barry CE, et al. Activation of c-Jun-N-terminal kinase is critical in mediating lipopolysaccharide-induced changes in the rat hippocampus. J Neurochem 2005;93:221–231. [PubMed: 15773921]

Beckham JD, et al. Novel strategy for treatment of viral central nervous system infection by using a cell-permeating inhibitor of c-Jun N-terminal kinase. J Virol 2007;81:6984–6992. [PubMed: 17475657]

Benn SC, Woolf CJ. Adult neuron survival strategies--slamming on the brakes. Nat Rev Neurosci 2004;5:686–700. [PubMed: 15322527]

Bifrare YD, et al. Bacterial meningitis causes two distinct forms of cellular damage in the hippocampal dentate gyrus in infant rats. Hippocampus 2003;13:481–488. [PubMed: 12836917]

Bifrare YD, et al. Brain-derived neurotrophic factor protects against multiple forms of brain injury in bacterial meningitis. J Infect Dis 2005;191:40–45. [PubMed: 15593001]

Borsello T, et al. A peptide inhibitor of c-Jun N-terminal kinase protects against excitotoxicity and cerebral ischemia. Nat Med 2003;9:1180–1186. [PubMed: 12937412]

Braun JS, et al. Neuroprotection by a caspase inhibitor in acute bacterial meningitis. Nat Med 1999;5:298–302. [PubMed: 10086385]

Brecht S, et al. Specific pathophysiological functions of JNK isoforms in the brain. Eur J Neurosci 2005;21:363–377. [PubMed: 15673436]

Cao J, et al. Distinct requirements for p38alpha and c-Jun N-terminal kinase stress-activated protein kinases in different forms of apoptotic neuronal death. J Biol Chem 2004;279:35903–35913. [PubMed: 15192112]

Carboni S, et al. Control of death receptor and mitochondrial-dependent apoptosis by c-Jun N-terminal kinase in hippocampal CA1 neurones following global transient ischaemia. J Neurochem 2005;92:1054–1060. [PubMed: 15715656]

Carboni S, et al. AS601245 (1,3-benzothiazol-2-yl (2-[[2-(3-pyridinyl) ethyl] amino]-4 pyrimidinyl) acetonitrile): a c-Jun NH2-terminal protein kinase inhibitor with neuroprotective properties. J Pharmacol Exp Ther 2004;310:25–32. [PubMed: 14988419]

Chang L, et al. JNK1 is required for maintenance of neuronal microtubules and controls phosphorylation of microtubule-associated proteins. Dev Cell 2003;4:521–533. [PubMed: 12689591]

Christen S, et al. Oxidative stress in brain during experimental bacterial meningitis: differential effects of alpha-phenyl-tert-butyl nitrone and N-acetylcysteine treatment. Free Radic Biol Med 2001;31:754–762. [PubMed: 11557313]

Cumming G, et al. Error bars in experimental biology. J Cell Biol 2007;177:7–11. [PubMed: 17420288]

Eilers A, et al. Direct inhibition of c-Jun N-terminal kinase in sympathetic neurons prevents c-jun promoter activation and NGF withdrawal-induced death. J Neurochem 2001;76:1439–1454. [PubMed: 11238729]

Eminel S, et al. c-Jun N-terminal kinases trigger both degeneration and neurite outgrowth in primary hippocampal and cortical neurons. J Neurochem. 2007

Gaillard P, et al. Design and synthesis of the first generation of novel potent, selective, and in vivo active (benzothiazol-2-yl)acetonitrile inhibitors of the c-Jun N-terminal kinase. J Med Chem 2005;48:4596–4607. [PubMed: 15999997]

Gerber J, et al. Increased neurogenesis after experimental Streptococcus pneumoniae meningitis. J Neurosci Res 2003;73:441–446. [PubMed: 12898528]

Gianinazzi C, et al. Caspase-3 mediates hippocampal apoptosis in pneumococcal meningitis. Acta Neuropathol (Berl) 2003;105:499–507. [PubMed: 12677451]

Gleeson JG, et al. Doublecortin is a microtubule-associated protein and is expressed widely by migrating neurons. Neuron 1999;23:257–271. [PubMed: 10399933]

Grandgirard D, et al. Pneumococcal meningitis induces apoptosis in recently postmitotic immature neurons in the dentate gyrus of neonatal rats. Dev Neurosci 2007;29:134–142. [PubMed: 17148956]

Grimwood K, et al. Adverse outcomes of bacterial meningitis in school-age survivors. Pediatrics 1995;95:646–656. [PubMed: 7536915]

Jin K, et al. Neurogenesis in dentate subgranular zone and rostral subventricular zone after focal cerebral ischemia in the rat. Proc Natl Acad Sci U S A 2001;98:4710–4715. [PubMed: 11296300]

Krawisz JE, et al. Quantitative assay for acute intestinal inflammation based on myeloperoxidase activity. Assessment of inflammation in rat and hamster models. Gastroenterology 1984;87:1344–1350. [PubMed: 6092199]

Kuan CY, et al. A critical role of neural-specific JNK3 for ischemic apoptosis. Proc Natl Acad Sci U S A 2003;100:15184–15189. [PubMed: 14657393]

Kuan CY, et al. The Jnk1 and Jnk2 protein kinases are required for regional specific apoptosis during early brain development. Neuron 1999;22:667–676. [PubMed: 10230788]

Leib SL, et al. Inhibition of matrix metalloproteinases and tumour necrosis factor alpha converting enzyme as adjuvant therapy in pneumococcal meningitis. Brain 2001;124:1734–1742. [PubMed: 11522576]

Loeffler JM, et al. The free radical scavenger alpha-phenyl-tert-butyl nitrone aggravates hippocampal apoptosis and learning deficits in experimental pneumococcal meningitis. J Infect Dis 2001;183:247–252. [PubMed: 11110643]

Manning AM, Davis RJ. Targeting JNK for therapeutic benefit: from junk to gold? Nat Rev Drug Discov 2003;2:554–565. [PubMed: 12815381]

Merkelbach S, et al. Cognitive outcome after bacterial meningitis. Acta Neurol Scand 2000;102:118–123. [PubMed: 10949529]

Mitchell L, et al. Dual phases of apoptosis in pneumococcal meningitis. J Infect Dis 2004;190:2039–2046. [PubMed: 15529270]

Nau R, et al. Apoptosis of neurons in the dentate gyrus in humans suffering from bacterial meningitis. J Neuropathol Exp Neurol 1999;58:265–274. [PubMed: 10197818]

Okuno S, et al. The c-Jun N-terminal protein kinase signaling pathway mediates Bax activation and subsequent neuronal apoptosis through interaction with Bim after transient focal cerebral ischemia. J Neurosci 2004;24:7879–7887. [PubMed: 15356200]

Papa S, et al. Linking JNK signaling to NF-kappaB: a key to survival. J Cell Sci 2004;117:5197–5208. [PubMed: 15483317]

Pfister LA, et al. Endothelin inhibition improves cerebral blood flow and is neuroprotective in pneumococcal meningitis. Ann Neurol 2000;47:329–335. [PubMed: 10716252]

Ren H, et al. Induction of haem oxygenase-1 causes cortical non-haem iron increase in experimental pneumococcal meningitis: evidence that concomitant ferritin up-regulation prevents iron-induced oxidative damage. J Neurochem 2007;100:532–544. [PubMed: 17116231]

Schaper M, et al. Cerebral vasculature is the major target of oxidative protein alterations in bacterial meningitis. J Neuropathol Exp Neurol 2002;61:605–613. [PubMed: 12125739]

Schuchat A, et al. Bacterial meningitis in the United States in 1995. Active Surveillance Team. N Engl J Med 1997;337:970–976. [PubMed: 9395430]

Sury MD, et al. Evidence that N-acetylcysteine inhibits TNF-alpha-induced cerebrovascular endothelin-1 upregulation via inhibition of mitogen- and stress-activated protein kinase. Free Radic Biol Med 2006;41:1372–1383. [PubMed: 17023264]

Waetzig V, Herdegen T. Context-specific inhibition of JNKs: overcoming the dilemma of protection and damage. Trends Pharmacol Sci 2005;26:455–461. [PubMed: 16054242]

Wakamatsu Y, Weston JA. Sequential expression and role of Hu RNA-binding proteins during neurogenesis. Development 1997;124:3449–3460. [PubMed: 9310339]

Weston CR, Davis RJ. The JNK signal transduction pathway. Curr Opin Cell Biol 2007;19:142–149. [PubMed: 17303404]

Xia Z, et al. Opposing effects of ERK and JNK-p38 MAP kinases on apoptosis. Science 1995;270:1326–1331. [PubMed: 7481820]

Yang DD, et al. Absence of excitotoxicity-induced apoptosis in the hippocampus of mice lacking the Jnk3 gene. Nature 1997;389:865–870. [PubMed: 9349820]

Zhuang ZY, et al. A peptide c-Jun N-terminal kinase (JNK) inhibitor blocks mechanical allodynia after spinal nerve ligation: respective roles of JNK activation in primary sensory neurons and spinal astrocytes for neuropathic pain development and maintenance. J Neurosci 2006;26:3551–3560. [PubMed: 16571763]

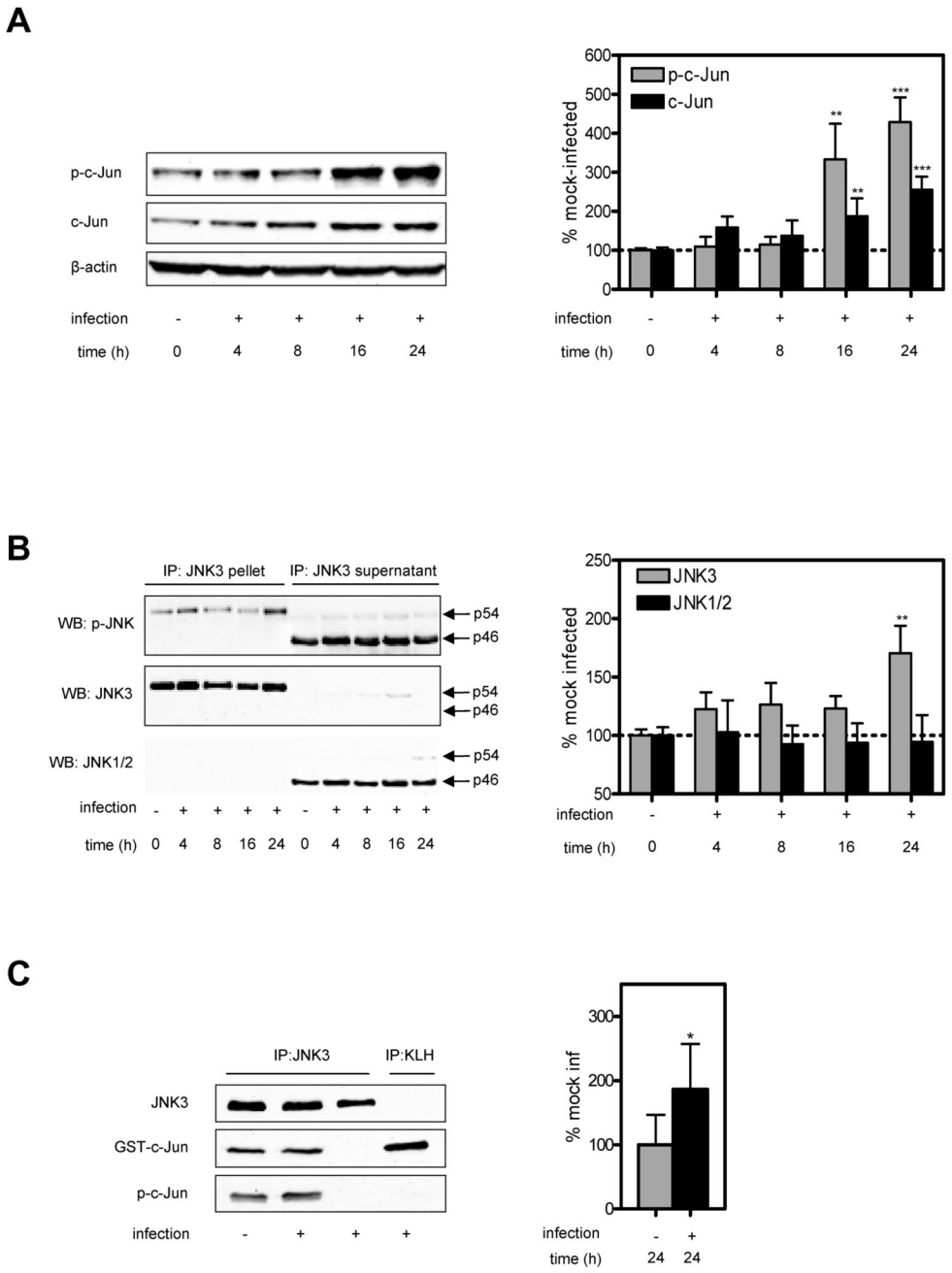

Figure 1. Kinetics of c-Jun phosphorylation, c-Jun protein expression, and isoform-specific analysis of JNK activation in the hippocampus

(A) Representative phospho-c-Jun (Ser73) and c-Jun Western blot. Reprobing with β-actin confirmed equal loading. Bar graph shows densitometric analysis of bands from 4–12 individual animals per time point expressed as the percentage of the mean ± SE of mock-infected animals (=100%). ***P*<0.01, ****P*<0.001 vs. control (indicated as t=0). **(B)** JNK3 immunoprecipitates and immunoprecipitation supernatant were probed for JNK phosphorylation in the conserved activation domain. Reprobing of the membrane with JNK3 and JNK1/2-specific antibodies was used for confirmation of isoform-specific immunoprecipitation. Representative blot shown. Bar graph shows densitometric analysis of

bands expressed as the percentage of the mean of mock-infected animals (=100%). Results show data from 5–8 individual animals per time point. ***P*<0.01. **(C)** In vitro kinase activity of JNK3 immunoprecipitates was assessed using GST-c-Jun as substrate. Activity was analyzed by measuring phosphorylation of GST-c-Jun using the Ser73 antibody. An anti-key limpet hemocyanin antibody (KLH) was used as negative control for immunoprecipitation. Bar graph shows densitometric analysis of phospho-GST-c-Jun corrected against JNK3 input. Results are expressed as the percentage of the mean of mock-infected animals (=100%) and represent data from 6 individual animals each. **P*<0.05 vs. mock-infected animals.

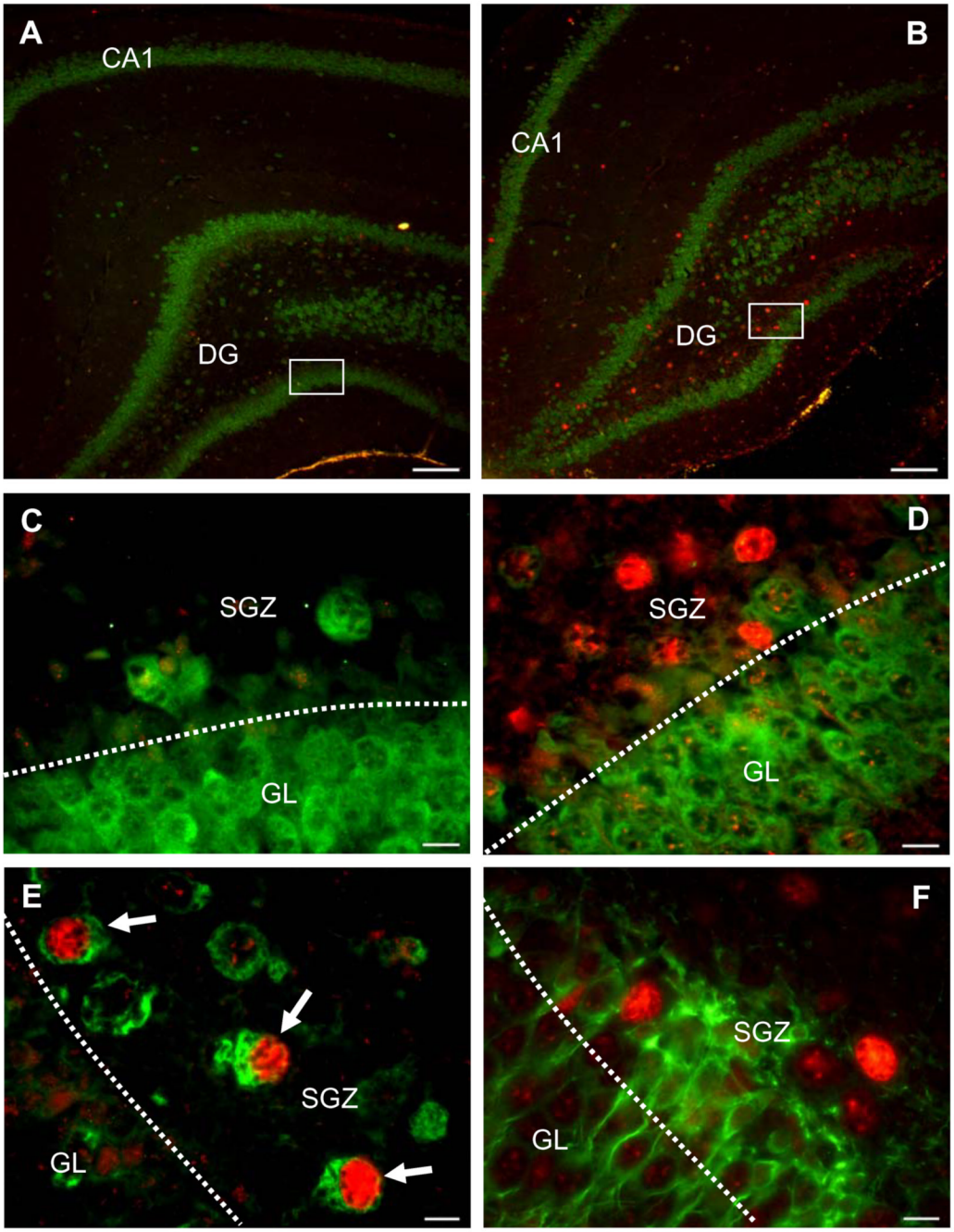

Figure 2. Cellular localization of c-Jun phosphorylation in the hippocampus of infected (B, D, E, F,) vs. mock-infected (A, C) animals

(A, B) Double-staining for phospho-c-Jun (red) and NeuN (green), a marker of mature neurons. Images show an overview of the dentate gyrus (DG) and cornu ammonis (CA) 1 region of the hippocampus. **(C, D)** Close-up view of phospho-c-Jun (red) and NeuN (green) double-staining in the dentate gyrus. Infection is associated with a marked increase of phospho-c-Jun in cells of the subgranular zone (SGZ) but not the granular cell layer (GL). **(E)** Phospho-c-Jun (red) and Hu (green) co-localization. Arrowheads indicate marked increase of phospho-c-Jun in early immature (Hu-positive) cells. **(F)** Lack of co-localization of phospho-c-Jun (red) with doublecortin (green)-positive cells (migrating neurons). **(A, B)** Scale bar, 100 μm, **(C-F)** scale

bar, 10 μm. Images are representative of staining obtained in sections prepared from at least 3 different animals per group.

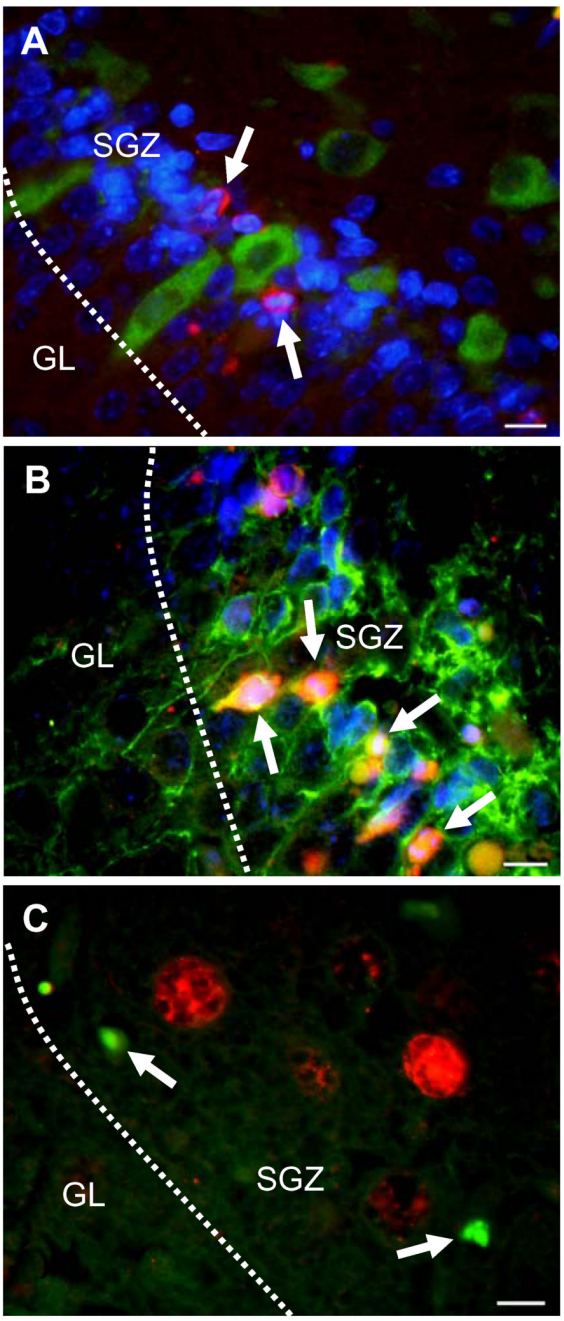

Figure 3. Characterization of apoptotic cells in the hippocampus of infected animals

(A, B) Triple staining for nuclei (blue), active caspase 3 (red), and developmental marker of immature neurons (green). Arrowheads point at morphologically apoptotic cells in the subgranular zone (SGZ) that are positive for active caspase 3. Active caspase 3-positive cells do not co-localize with Hu **(A)**, but with doublecortin **(B)**. **(C)** Arrowheads point at TUNEL-positive cells (green), which do not co-localize with phospho-c-Jun-positive cells (red). Images are representative of staining obtained in sections prepared from at least 3 different animals for each treatment group. Scale bar, 10 μm.

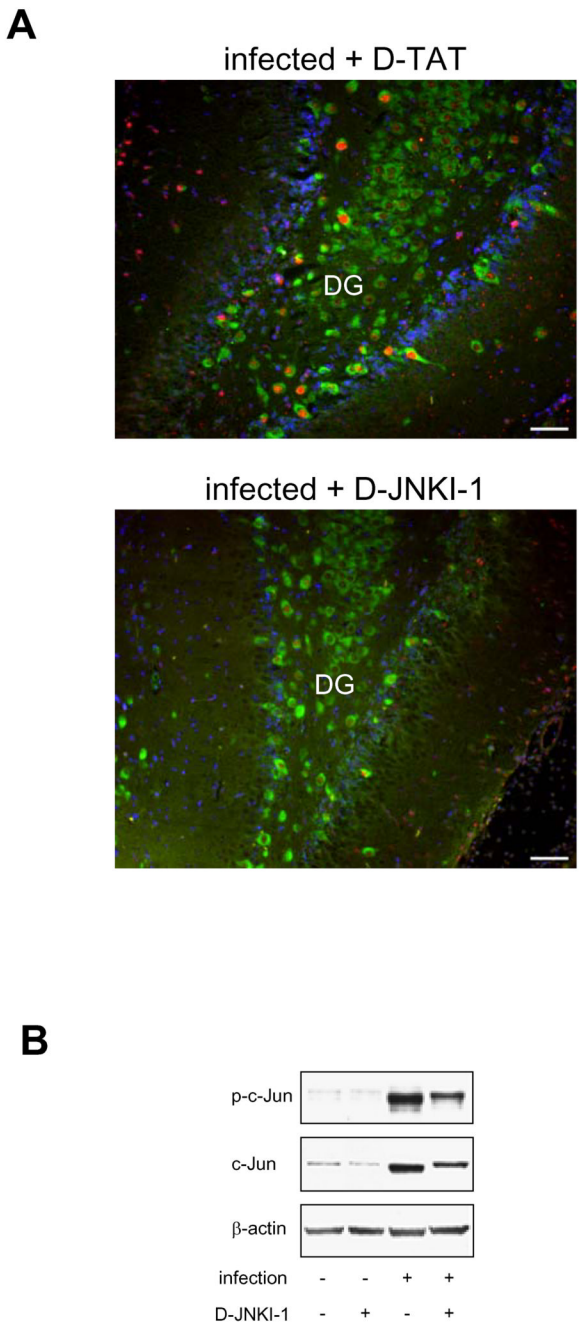

Figure 4. Effect of D-JNKI-1 on c-Jun phosphorylation and c-Jun protein expression

Analyses were performed in the hemisphere contralateral to the one used for counting apoptosis. **(A)** Representative images showing that D-JNKI-1 inhibits increased infection-induced c-Jun phosphorylation (red) in Hu-positive neurons (green) of the dentate gyrus (DG). Nuclei are stained with DAPI (blue). Scale bar, 50 μm. Images are representative of staining obtained in sections prepared from at least 3 different animals for each treatment group. **(B)** Representative phospho-c-Jun and c-Jun Western blot of D-JNKI-1 and vehicle (D-TAT)-treated animals. Numeric evaluation of Western blot data is described in text.

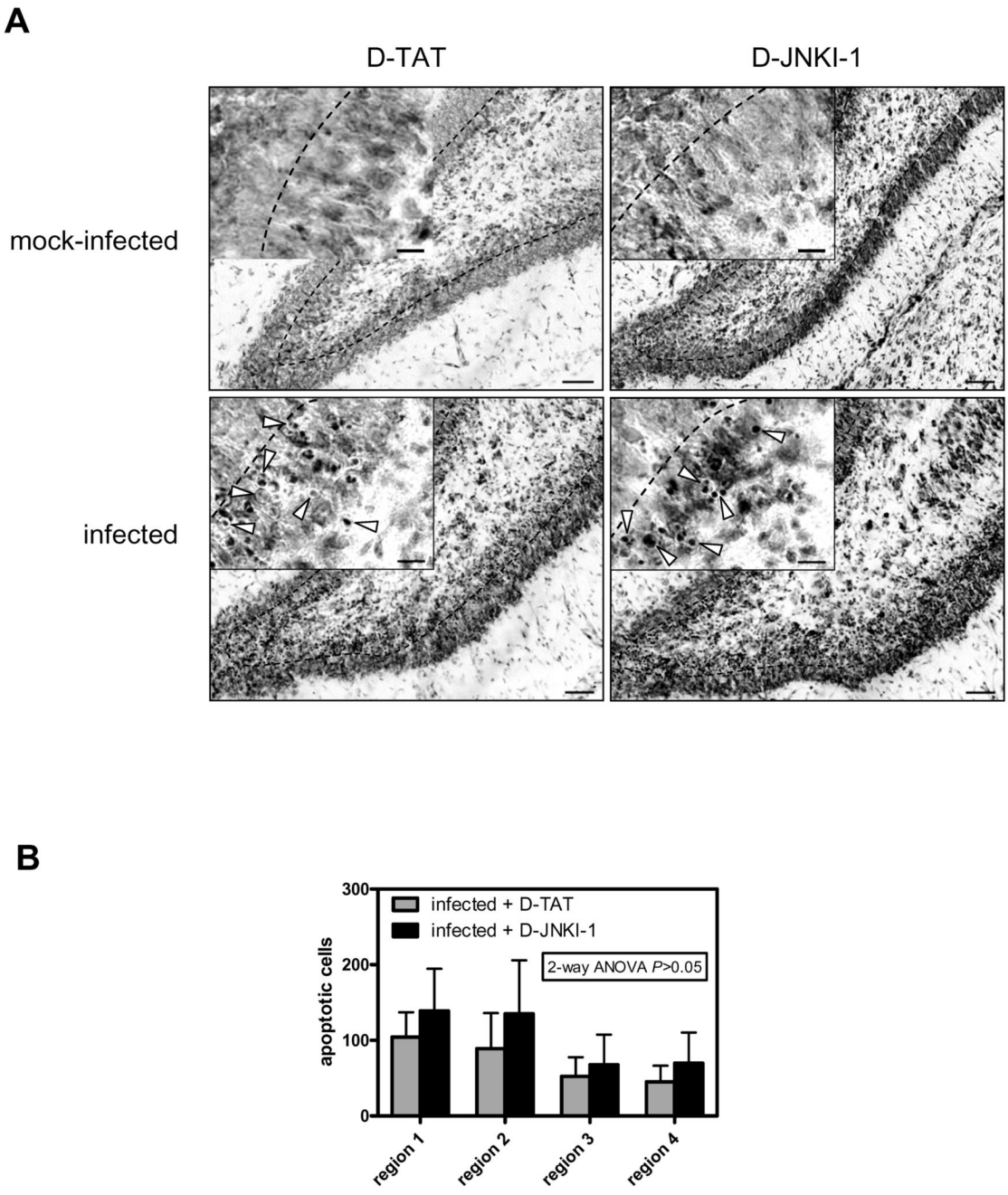

Figure 5. Effect of D-JNKI-1 on hippocampal apoptosis

(A) Images show cresyl violet stained sections of the denate gyrus of either vehicle (D-TAT) or D-JNKI-1-treated mock-infected (top) or infected animals (bottom). Scale bar 50 μm. Arrowheads in the close up view point at cells with apoptotic morphology (condensed fragmented dark nuclei / apoptotic bodies). Scale bar 10 μm. **(B)** Evaluation of apoptosis in the dentate gyrus of cresyl violet-stained sections of D-JNKI-1-treated (n=9) vs. vehicle-treated (n=9) infected animals. Results are presented as the mean ± SD of the morphologically apoptotic cells in the 4 different regions of the dentate gyrus (region 1–4, from anterior to posterior). There was neither a significant effect of DJNKI-1 on apoptosis overall (2-way ANOVA) nor in the individual regions (Bonferroni post-hoc test).

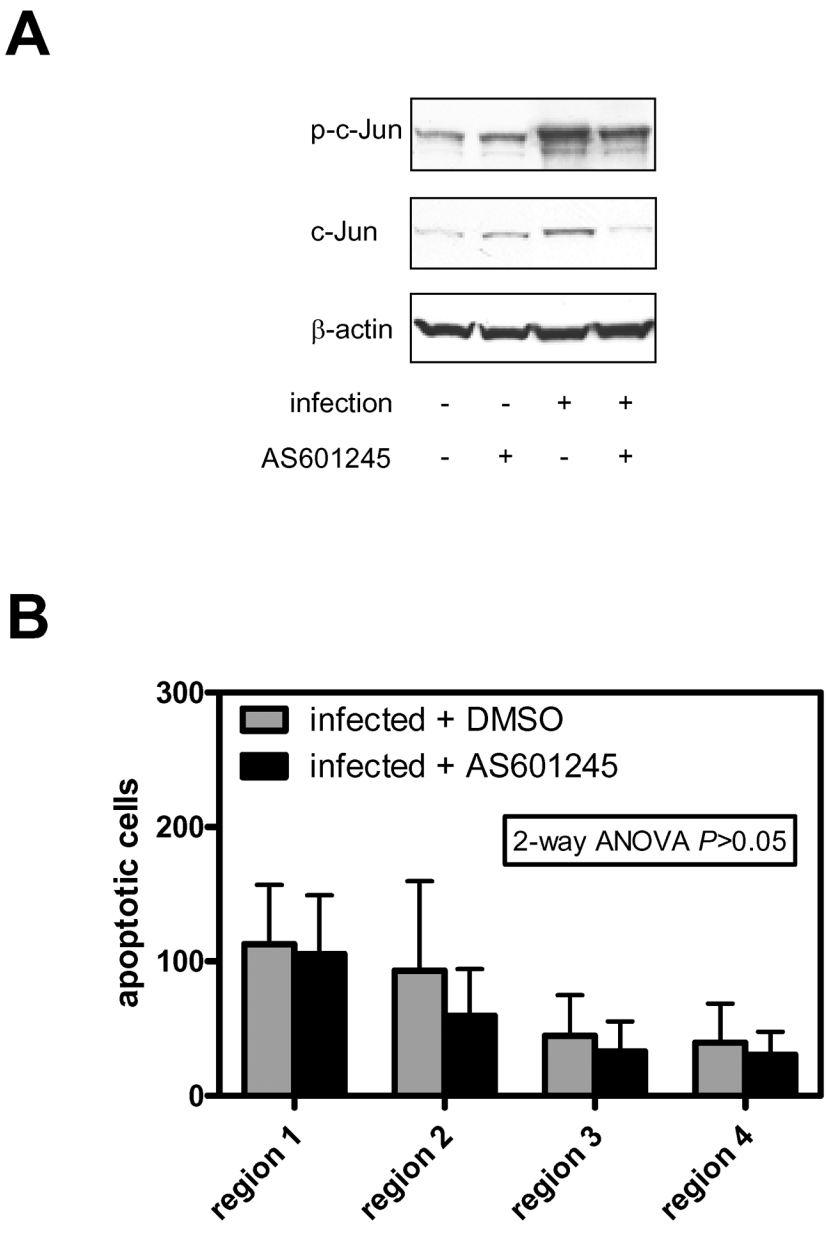

Figure 6. Effect of AS601245 on c-Jun phosphorylation, c-Jun protein expression and hippocampal apoptosis

(A) Representative phospho-c-Jun and c-Jun Western blot of AS601245 and vehicle (DMSO)-treated animals. **(B)** Evaluation of apoptosis in the dentate gyrus of cresyl violet-stained sections of AS601245-treated (n=9) vs. vehicle-treated (n=9) infected animals. Results are presented as the mean ± SD of the morphologically apoptotic cells in the 4 different regions of the dentate gyrus (region 1–4, from anterior to posterior). There was neither a significant effect of AS601245 on apoptosis overall (2-way ANOVA) nor in the individual regions (Bonferroni post-hoc test).

Table1

Lack of effect of JNK inhibition on clinical course of infection

treatment	D-JNKI-1 (4 nmol)		AS601245 (200 nmol)	
	Vehicle (D-TAT)	inhibitor	Vehicle (DMSO)	inhibitor
CSF bacterial titer (log cfu/ml)	8.41 ± 1.16 (*13*)	8.41 ± 1.39 (*12*)	7.50 ± 0.47 (*11*)	7.26 ± 0.51 (*10*)
clinical score	3.9 ± 0.49 (*13*)	4.0 ± 0.00 (*15*)	4.1 ± 0.75 (*13*)	4.1 ± 0.99 (*15*)
weight loss (g)	0.58 ± 0.97 (*13*)	0.60 ± 1.50 (*15*)	0.92 ± 1.12 (*13*)	1.60 ± 0.77 (*15*)
CSF MPO activity (%infected)	100.0 ± 12.6 (*8*)	100.4 ± 18.2 (*13*)	100.0 ± 13.2 (*8*)	108.4 ± 38.2 (*6*)

CSF bacterial titer, clinical score and MPO activity in CSF cell pellets were determined at 18 h p.i., whereas weight loss was determined at 24 h p.i. In comparison, mock-infected animals gain 2 to 3 g of body weight within this time period. Results represent mean ± SD of number of animals indicated in brackets, with the exception of the MPO data, which are expressed relative to the V max of vehicle-treated animals (mean ± SE). No significant differences between inhibitor-treated animals and their respective vehicle-treated controls by Student t-test.